MERLIN-DEFICIENT iPSCs SHOW ALTERED PLURIPOTENCY AND CONSTITUTE A POTENTIAL *IN VITRO* MODEL FOR NF2-RELATED SCHWANNOMAS

Núria Catasús[1], Miguel Torres-Martin[1,2], Alex Negro[1,2], Bernd Kuebler[3], Inma Rosas[1,2], Gemma Casals[1], Helena Mazuelas[4], Francesc Roca-Ribas[5], Emilio Amilibia[5], Begoña Aran[3], Anna Veiga[3], Ángel Raya[3], Bernat Gel[4], Ignacio Blanco[1,2], Eduard Serra[4*], Meritxell Carrió[4*] and Elisabeth Castellanos[1,2*]

*Equally contributed

1) Clinical Genomics Research Group, Germans Trias i Pujol Research Institute (IGTP); Can Ruti Campus, Badalona, Barcelona, Spain
2) Clinical Genomics Unit, Germans Trias i Pujol University Hospital (HUGTiP), Can Ruti Campus, Badalona, Barcelona, Spain
3) Medicine Regenerative Program, Institut d'Investigació Biomèdica de Bellvitge. IDIBELL, Hospital Duran i Reynals, Gran Via de L'Hospitalet, 199-203, 08908, L'Hospitalet de Llobregat, Barcelona, Spain.
4) Hereditary Cancer Group, Germans Trias i Pujol Research Institute (IGTP); Can Ruti Campus, Badalona, Barcelona, Spain
5) Otorhinolaryngology Department, Germans Trias i Pujol University Hospital (HUGTiP), Can Ruti Campus, Badalona, Barcelona, Spain

Corresponding author: Eduard Serra (eserra@igtp.cat); Meritxell Carrió (mcarriol@igtp.cat); Elisabeth Castellanos (ecastellanos@igtp.cat/ecastellanosp.germanstrias@gencat.cat)

Abstract

Background: The appearance of bilateral vestibular schwannomas (VS) is one of the most characteristic features of NF2-related schwannomatosis (NF2-related SWN), an autosomal dominant syndrome that predisposes to the development of tumours of the nervous system. VS are caused by the bi-allelic inactivation of the NF2 gene in a cell of the Schwann cell lineage. Our current understanding of VS initiation and progression as well as the development of new effective therapies is hampered by the absence of human non-perishable cell-based models.

Principal Findings: We generated and characterized induced pluripotent stem cell (iPSC) lines with single or bi-allelic inactivation of *NF2* by combining the direct reprogramming of VS cells with the use of CRISPR/Cas9 editing. Despite the difficulty of maintaining merlin-deficient iPSCs, we were able to differentiate them into neural crest (NC) cells. At this stage, these cells showed

spontaneous expression of the SC marker S100B and the impossibility of generating Schwann cells in 2D cultures. Nevertheless, by applying a 3D Schwann cell differentiation protocol, we successfully generated *NF2*(+/-) and *NF2*(-/-) spheroids homogeneously expressing classical markers of the NC-SC axis.

Conclusions: Our results show a critical function of *NF2* for both reprograming and maintaining a stable pluripotent state. In addition, merlin-deficient cultures also denoted an altered differentiation capacity of merlin-deficient cells towards the NC-SC axis, in the *in vitro* conditions used. Finally, the generated *NF2*(+/-) and *NF2*(-/-) spheroids show potential as a genuine in vitro model of NF2-related tumours.

Keywords: Neurofibromatosis Type 2; iPSC; Schwann Cell; Neural crest stem cell; Vestibular Schwannomas, Schwannomas

52 **Introduction**

53 NF2-related schwannomatosis (NF2-related SWN; OMIM 101000) is a dominantly inherited
54 autosomal syndrome characterized by the development of multiple tumours of the nervous
55 system (1,2). This condition is caused by pathogenic variants in the *NF2* tumour suppressor
56 gene (22q12.2), which codes for merlin (moesin-ezrin-radixin-like protein); a scaffold protein
57 that interacts with transmembrane receptors and intracellular effectors to mediate mitogenic,
58 survival and cell-cell contact signalling pathways. Changes in merlin result in the inhibition of
59 cell proliferation (3–5). The incidence of the disease is estimated at 1:28.000 live births with a
60 complete penetrance by the age of 60, with 50–60% of cases being due to *de novo* mutations
61 (6). The pathognomonic feature of the disease is the development of bilateral vestibular
62 schwannomas (VS), well-circumscribed intracranial tumours attached to the vestibulocochlear
63 nerve that arise from Schwann Cells (SC) as a result of the bi-allelic *NF2* inactivation. Affected
64 individuals may also develop multiple schwannomas in other cranial, spinal and peripheral
65 nerves as well as intracranial and intraspinal meningiomas, and spinal ependymomas (7–10).
66 Cutaneous and ocular manifestations are also frequent (11,12). Although histologically benign,
67 these tumours are responsible for high morbidity and a reduced life expectancy due to their
68 number and anatomical location (13).

69 VS naturally grow over time (9,14–16) and are responsible for significant morbidity associated
70 with NF2-related SWN, which includes hearing loss, deafness and tinnitus that can eventually
71 progress to facial paraesthesia, ataxia and vertigo (17). The gold standard for treatment of VS
72 include surveillance, surgery, radiotherapy and Bevacizumab (17). The latter, an anti-VEGF
73 monoclonal antibody, that has been shown to induce reduction of tumour growth and an
74 improvement in hearing loss in NF2-related SWN patients, although with associated toxicity
75 when sustained over time (18). However, the remaining therapeutic options also present
76 different adverse effects, for example, the resection of VS often results in hearing loss,
77 patients then requiring cochlear or brainstem implants to preserve hearing whereas,

78 radiotherapy of these tumours has been shown to induce tumour malignancy over time
79 (19,20). For the reasons above, efforts have been made to develop alternative therapies for
80 NF2-related tumours, such as Losartan (antihypertensive), Lapatinib (tyrosine kinase inhibitor)
81 or AR-42 (Histone deacetylase (HDAC) inhibitor) (21–24). However, since the disease course for
82 these tumours can be extremely long, there is a need to develop novel treatments with
83 minimal side effects.

84 The study of the role of *NF2* in VS development and progression, and the development of
85 potential therapies, is still challenging due to the lack of non-perishable preclinical models that
86 reproduce patient genetics and the pathophysiology of NF2-related tumours. The first
87 attempts to generate *in vivo* murine models revealed the essentiality of *NF2* during
88 embryogenesis and early development (19). While homozygous *NF2* mutant mice fail to
89 develop vital extraembryonic structures, which impedes them from reaching a gastrulation
90 stage, mosaic *NF2*(-/-) embryos show defects in a variety of other embryonic tissues (19). In
91 *NF2*(+/-) mutant mice, the deficiency of a single *NF2* allele causes the appearance of malignant
92 epithelial tumours and sarcomas with an aggressive tendency to metastasize (25). (25).
93 Conditional KO murine models can generate schwannomas and, in some cases VS, although
94 histologically they differ from human schwannomas (26,27). In addition, several xenograft
95 mouse models have also been developed, with different levels of success in recapitulating the
96 biology of human NF2-related SWN traits (28).

97 *In vitro*, primary SC cultures derived from VS have been established and demonstrated to
98 preserve the pathophysiology of the tumour (29,30). However, the limited lifespan of primary
99 cultures can severely constrain their use for extended experiments, or when large numbers of
100 cells are required. Transformed and immortalized VS derived cell lines have been developed in
101 order to overcome this limitation, and have been widely used as platforms for drug screening
102 (HEI-93, JEI-001) (31,32), although these models may undergo physiological changes due to the
103 immortalisation process, severely reducing the value of any comparison with primary cells.

104 Induced pluripotent stem cell (iPSC) (33) models have been used in a wide range of diseases,
105 representing an unlimited source of cells with diverse applications such as disease modelling,
106 drug development, regenerative medicine or gene regulation (34–37). The first related model
107 reported for NF2-related SWN was an iPSC line harbouring a homozygous variant in the *NF2*
108 gene (UMi031-A-2), obtained through gene editing by CRISPR/Cas9 of a non-affected
109 pluripotent cell line (38); and more recently, an iPSC clone has been derived from mononuclear
110 bone marrow-derived stem cells of a mosaic NF2-related SWN patient (39). However, there is
111 still the need to develop relevant disease models from these iPSC, which fully recapitulate the
112 genetic and physiological status of *NF2* derived VS.
113 One of the main defining characteristics of iPSC is that they have the ability to differentiate to
114 the three germ layers. Protocols have been developed to differentiate iPSC towards the SC
115 lineage, passing through an intermediate multipotent neural crest stage (40–42). It has been
116 shown that when applying these protocols, iPSC-derived SCs show homogenous expression of
117 SC markers and have the capacity to myelinate axons when they are co-cultured with dorsal
118 root ganglia neurons (42). Therefore, the use of iPSC seems to represent a suitable human SC-
119 based cellular model to study the molecular pathogenesis of NF2-related schwannomas.
120 In the present study we have generated iPSC lines harbouring single or bi-allelic loss of
121 function variants in the *NF2* gene by direct reprogramming of VS cells and the use of
122 CRISPR/Cas9 editing. These cells were characterized and differentiated towards the NC-SC
123 lineage, obtaining *NF2*(+/-) and *NF2*(-/-) spheroids that co-express classical markers of the NC-
124 SC axis, thereby potentially representing a bona fide NF2-related schwannoma model.
125
126 **Results**
127 **1. Generation of induced pluripotent stem cells harbouring single or bi-allelic mutations**
128 **in the *NF2* gene**

129 Three VS from NF2-related SWN patients that met standard diagnostic criteria (43) were used
130 for reprogramming (VS-25, VS-245 and VS-267). Molecular characterization of these tumours
131 through the I2HCP panel (44) uncovered the *NF2* alterations reported in Supplemental Table
132 S1. In addition, no pathogenic variants were identified in known oncogenes or tumour
133 suppressor genes, as has been previously reported for VS. SNP-array analysis showed loss of
134 heterozygosity (LOH) on chromosome 22q in VS-25, and no complex rearrangements were
135 observed in any of the tumours analysed (Supplemental Figure S1).
136 The non-integrating Sendai virus vector (SeV) encoding the 4 Yamanaka factors (33) was used
137 to induce pluripotency of VS-dissociated cells, with the aim of generating iPSC *NF2*(-/-) clones
138 that could recapitulate the genetic background of Schwann cells involved in VS tumorigenesis.
139 After VS reprogramming, we determined the *NF2* genotype through Sanger sequencing of 38
140 single-cell clones for VS-25, 12 for VS-267 and 10 for VS-245 (Supplemental Table S2). From VS-
141 25 and VS-267, only clones carrying the germline *NF2* pathogenic variant, *NF2*(+/-), were
142 obtained. One of these clones derived from each tumour was selected for further
143 characterization. From VS-245, a tumour coming from a mosaic patient, we obtained both
144 *NF2*(-/-) and *NF2*(+/+) iPSC clones. As VSi-245(+/+) clones were reprogrammed from an
145 unaffected cell, these were not further characterized. We focused on characterizing *NF2*(-/-)
146 clones that were already distinctive in culture due to their aberrant morphology, containing
147 cells that were piling up on top of others (Supplemental Figure S2). Surprisingly, all VSi-245
148 *NF2*(-/-) iPSC clones (n=9), proved to be dependent on the exogenous expression of Yamanaka
149 factors by the Sendai (SeV) construct. Although SeV is a non-integrating RNA virus widely used
150 for reprogramming, the expression of which is commonly lost due to dilution of the viral
151 genome, *NF2*(-/-) clones could only be established directly from VS in the presence of SeV, this
152 remained true 40 passages after reprogramming, or after submitting the iPSC clones to 39°C
153 for several passages to achieve complete clearance of the virus. These clones showed
154 sustained expression of reprogramming factors (Supplemental Figure S2). Therefore, we

155 concluded that these clones could not constitute a reliable model and were discarded for the

Table 1. iPSCs lines information

156 rest of the study.

157 Genomic characterization of *NF2*(+/-) VSi-25 and VSi-267 iPSCs selected clones by SNP-array
158 analysis and WES showed no differences with respect to the tumour of origin, with a logical
159 exception for VSi-25, in which the LOH on chromosome 22q as the second hit was not present
160 in the (+/-) clones obtained from this tumour (Supplemental Figure S1).

161 With the aim of achieving iPSCs with complete *NF2* inactivation, and given the low efficiencies
162 obtained and the SeV dependency in the generation of *NF2*(-/-) clones through
163 reprogramming, we decided to use CRISPR/Cas9 technology to edit the *NF2* gene in both, the
164 *NF2*(+/-) clones obtained from reprogrammed VS cells and a control *NF2*(+/+) iPSC line (FiPS
165 Ctrl 1-SV4F-7, registered in the Spanish National Stem Cell Bank/ ESiO44C in
166 https://hpscreg.eu/)). Thus, using CRISPR/Cas9 RNP complexes, we targeted exon 2 of the *NF2*
167 gene and obtained several single-cell *NF2*(-/-) iPSC clones from VS-derived lines (named 25-
168 CasD7, when derived from VSi-25, and 267-CasD2 when derived from VSi-267) and isogenic
169 *NF2*(+/-) and *NF2*(-/-) iPSC clones derived from the control line (named FiPS-CasB2 and FiPS-
170 CasH6, respectively). Pathogenic variants in *NF2* were fully characterized through PCR and
171 Sanger sequencing and for each of them, the *NF2* coding region was cloned to confirm
172 compound heterozygous clones (Table 1). In addition, WES analysis of the edited lines revealed
173 no pathogenic off-target alterations (Supplemental Table S3).

174 From this point on, we worked on the characterization of six iPSC lines: three with one
175 pathogenic variant in *NF2* (two VS-reprogrammed and one control iPSC-edited) and three
176 carrying the bi-allelic inactivation of *NF2* (Table 1).

Generation method	Reprogramming VS		Editing iPSCs from VS		Editing FiPS Ctrl 1-SV4F-7	
iPS Cell line	**VSi-25**	**VSi-267**	**VSi-25-CasD7**	**VSi-267-CasD2**	**FiPS-CasB2**	**FiPS-CasH6**
***NF2* Genotype**	c.1736A>G	c.784C>T	Allele A: c.211dupA	c. 212_213delCA	c.212_213 delCA	c.211dupA
	WT ***NF2* (+/-)**	WT ***NF2* (+/-)**	Allele B: c.212_213delCA and c.1736A>G ***NF2* (-/-)**	c.784C>T ***NF2* (-/-)**	WT ***NF2* (+/-)**	c.212_213 delCA ***NF2* (-/-)**
p.	p.(Lys529Asnfs*19)	p.(Arg262*)	Allele A: p.(Thr71Asnfs*15) Allele B: p.(Thr71Serfs*14) p.(Lys529Asnfs*19)	p.(Thr71Serfs*14) p.(Arg262*)	p.(Thr71Serfs*14)	p.(Thr71Asnfs*15) p.(Thr71Serfs*14)
Effect	Splicing	Truncating	Splicing and truncating	Truncating	Truncating	Truncating
	NF2 (+/-)	*NF2* (+/-)	*NF2* (-/-)	*NF2* (-/-)	*NF2* (+/-)	*NF2* (-/-)
Affected exons	15	8	2 and 15	2 and 8	2	2

iPSCs: induced pluripotent stem cell; VS: vestibular schwannoma; FiPS; fibroblasts induced pluripotent stem cell; Ctrl: Control; WT: wild-type

2. *NF2* is necessary for maintaining a stable pluripotent state

The combination of strategies between VS reprogramming and *NF2* gene editing allowed us to obtain clones with single (+/-) or double (-/-) mutations in the *NF2* gene (Figure 1A). All of them expressed cell surface proteins and transcription factors associated with pluripotency: Oct4, SSEA-3, SSEA-4, Nanog, Sox2, Tra-1-60 and Tra-1-81; were positive for alkaline phosphatase staining; and showed karyotype stability after at least 20 passages (46, XY) (Supplemental Figure S3). In addition to the constitutional and somatic *NF2* mutation characterization (Table 1), we confirmed all *NF2* genotypes by performing western blot of merlin (Figure 1B). *NF2*(+/-) cell lines exhibited an approximately 50% reduction in merlin expression compared to the control and *NF2*(-/-) iPSCs showed no expression of the protein

191 (Figure 1B). Although all iPSC clones expressed the typical pluripotent markers, we could
192 observe differences in clone morphology between *NF2*(+/-) and *NF2*(-/-) cell lines. Whereas
193 *NF2*(+/-) showed classical iPSC colony morphology, edited *NF2*(-/-) iPSC colonies presented less
194 compact colony formation, eventually aggregating in the centre of the colony and growing
195 upwards and undergoing major spontaneous differentiation compared with the iPSC control
196 line (Figure 1C), as we had previously observed for the reprogrammed *NF2*(-/-) iPSC line.
197 Notably, the 267-CasD2 line required removal of visibly differentiated cells before each
198 passage. Furthermore, the three *NF2*(+/-) iPSC lines showed the capacity to differentiate into
199 the three primary germ layers *in vitro* (mesoderm, endoderm and ectoderm) through
200 embryoid body (EBs) formation (Figure 1D). In contrast, *NF2*(-/-) clones showed a unique
201 response. For the FiPS-CasH6 line, only EBs thrived under conditions of differentiation to
202 ectoderm and stained positive for TUJ1 and GFAP markers, but they did not achieve
203 differentiation to endoderm. In addition, differentiation through EBs did not succeed for the
204 25-CasD7 and 267-CasD2 lines applying standard protocols. After attempting differentiation
205 through EBs formation, direct differentiation protocols were used. Positive staining for some
206 markers of the three primary germ layers was achieved, although the morphology of iPSCs and
207 their derivatives was abnormal (Figure 1D, Supplemental Table S4), indicating again that loss of
208 *NF2* affects the pluripotency capacity of iPSCs. These observations, together with the data
209 previously compiled from VS cell reprogramming (low efficiency in the generation of *NF2*(-/-)
210 clones; dependency on SeV-expressed Yamanaka factors) and the phenotypic characteristics of
211 *NF2*(-/-) iPSC clones, suggest a critical role of the *NF2* gene in the maintenance of a
212 pluripotency state.
213
214 **Figure 1. Absence of merlin in iPSCs results in an altered pluripotent phenotype.** (A)
215 Schematic representation of the experimental procedure for obtaining merlin-null clones. (B)
216 Morphology of the cell colonies, Scale bar, 75µM; (C) Immunochemistry to demonstrate the

217 capacity of the lines to *in vitro* differentiate to the three primary germ layers of *NF2*(+/-) lines:
218 mesoderm (ASMA in green and ASA in red), ectoderm (TUJ1 in green and GFAP in red) and
219 endoderm (AFP in green and FOXA2 in red). For NF2(-/-), a directed differentiation was
220 performed due to the inability of these lines to generate EBs, for these: mesoderm (ASMA in
221 green and GATA4 in red), ectoderm (TUJ1 in green, GFAP in red and PAX6 in pink) and
222 endoderm (AFP in green, FOXA2 and SOX17 in red). Scale bar, 75µM (D) Merlin expression
223 analysed by Western Blot. The FiPS line generated from fibroblasts (NF2 +/+) was used as a
224 control cell line, NPE stands for Normalized Protein Expression.
225

226 **3. Merlin-deficient iPSCs have an altered capacity to acquire and retain a stable neural**
227 **crest identity**

228 The next step in the development of an iPSC-based VS model was their differentiation into
229 neural crest (NC) cells, previous to a final differentiation towards SCs. To generate NCs, we
230 applied chemically defined differentiation conditions as previously reported [41], containing
231 activators of the Wnt signaling pathway and inhibitors of the TGFβ/activin/nodal pathway.
232 During the first ten days after the induction of NC differentiation, cell morphology shifted and
233 achieved a NC morphology in all cell lines tested (Figure 2A). Cell identity was first assessed by
234 flow cytometry of NC markers, NGFR (p75) and HNK1 (CD57), at early passages of the NC
235 differentiation process (p4) and in a mature NC state (p8) (Figure 2B). In our hands, *NF2*(+/-)
236 NC cell lines, derived either from reprogrammed VS cells or edited from isogenic control (FiPS-
237 CasB2), showed around 90% of cells expressing both markers in a similar way to, but a bit less
238 efficiently than the *NF2*(+/+) control line. Distinctively, *NF2*(-/-) cell lines already showed some
239 expression of p75 and Hnk1 already at the iPSC stage, but did not acquired the same
240 percentages of p75/Hnk1 positive cells at the mature NC stage, with an average of 76,3% for
241 the three cell lines (Figure 2B).

242 NC identity was further characterized through immunocytochemistry and transcriptome
243 analysis (RNA-seq), showing that all cell lines, *NF2* (+/+), (+/-) and (-/-), expressed the NC
244 markers Sox10, TFAP2A and p75 and showed no expression of the pluripotency markers
245 POU5F1 (Oct4), Nanog and Sox2 (Figure 2C and 2D). However, some *NF2*(-/-) NC cells were also
246 expressing S100B both at the RNA and protein levels (Figure 2C and 2D), which was consistent
247 with the heterogeneity detected by flow cytometry assays. Differences in merlin-deficient NC
248 cells were also observed in culture conditions, as these cells required culturing at higher cell
249 confluence conditions, compared to *NF2*(+/+) or *NF2*(+/-), to maintain a NC cell morphology.
250 Despite these differences, all generated lines were able to maintain a self-renewal capacity for
251 at least 18 passages while preserving a NC identity, and could be cultured after several freeze-
252 thaw cycles.
253 In summary, *NF2*(+/-) and *NF2*(-/-) iPSC lines could be differentiated towards a NC identity.
254 However, generation of *NF2*(-/-) NC cultures was less efficient, required special care to
255 maintain a NC morphology, and the resulting *NF2*(-/-) NC population expressed both NC
256 markers but also the S100B SC marker, suggesting that *NF2* function is important to acquire
257 and retain a stable neural crest identity.
258
259 **Figure 2. Neural Crest Characterization.** (A) NC Morphology of *NF2*(+/-) and *NF2*(-/-) cell lines;
260 Scale bar, 75µM; (B) Flow cytometry assays of the NC markers NGFR (p75) and Hnk1. The
261 percentage of p75 and Hnk1-positive cells is shown in pink. P4 and P8 stand for passages 4 and
262 8, respectively; (C) Immunocytochemistry of AP2 (green), p75 (green) and S100B (red), Scale
263 bars, 25µM; Oct4 (green) and SOX10 (red), Scale bar, 100µM; DAPI (blue) was used to stain cell
264 nuclei. (D) Expression levels of the genes related to a pluripotent stage (Nanog and Sox2), a NC
265 stage (Sox10 and AP2) and a SC marker (S100). Y-axis represents normalized FPKM expression.
266
267 **4. Schwann Cell Differentiation of *NF2*(+/-) and *NF2*(-/-) from derived-NC cultures**

268 A final step consisted in inducing the differentiation of the established NC cultures towards a
269 SC state. Thus, NCs were cultured in SC differentiation medium (SCDM) for 30 days, as
270 previously stablished [41]. During the differentiation process, significant differences were
271 observed between *NF2*(+/+) control and merlin-deficient cell lines: five days after inducing SC
272 differentiation, *NF2*(+/-) and *NF2*(-/-) cell lines showed difficulties in maintaining adherence to
273 culture dishes, in contrast to the control line, which after seven days already showed a more
274 elongated spindle morpohlogy resembling SC-like cells (Supplemental Figure S5). Expression
275 analysis indicated that *NF2*(+/+) NC cultures in 2D were able to differentiate towards a
276 Schwann cell lineage, as they expressed classical NC-SC lineage markers and also the NC-SC
277 roadmap gene signature described in Mazuelas et al (2022) (Supplemental Figure S6) (45). In
278 contrast, we reasoned that the poor adherence capacity of merlin-deficient NCs compromised
279 their ability to differentiate towards a SC identity. Consequently, we tested the SC
280 differentiation capacity of these cells in 3D cultures, following a previously established
281 protocol (45) with minor modifications. In brief, NC cells were seeded in uncoated spheroid
282 AggreWell plates for up to 30 days in SC differentiation medium. This procedure was
283 monitored at three time points (7, 14 and 30 days) through immunocytochemistry and RNA-
284 seq analysis (Figure 3). We used *NF2*(+/+) differentiating cells as an experimental control. At
285 the RNA level, we observed that *NF2*(+/+) differentiating spheroids expressed typical lineage
286 markers (S100B, MPZ or PLP1) already at day 7, which were maintained after 14 days under
287 SCDM. The expression of SC markers was not equally sustained up to 30-days of differentiation
288 (Supplementary Figure S7), indicating that this differentiation protocol was most appropriate
289 up to 14 days of differentiation. *NF2*(+/+) spheroids were also positive for p75 and S100B
290 markers identified by immunostaining (Figure 3A). Then, we differentiated *NF2* mutant cell
291 lines in these conditions. Both *NF2*(+/-) VSi-25 and VSi-267 cell lines formed spheroids that
292 stained positive for p75 and S100B markers, as well as the three *NF2*(-/-) cell lines (Figure 3A).

293 However, unexpectedly we were unable to obtain spheroids from the edited FiPS-CasB2
294 *NF2*(+/-) cell line (Supplemental Figure S8).
295 In order to determine the SC differentiation capacity of *NF2*(+/-) and (-/-) cell lines, we studied
296 the transcriptome of the whole differentiation process. First we performed a principal
297 component analysis (PCA) of all cell lines, including the iPSC and NC stages and throughout the
298 SC differentiation process (Figure 3B). Cells at different differentiation stages clustered
299 together, indicating that we were able to reliably distinguish between the three cell types. All
300 iPSC cells grouped together, although the edited *NF2*-deficient 267-CasD2 line positioned
301 slightly apart from the rest. Also, all SCs differentiating in 3D clustered together independently
302 of the genotype or days of differentiation (Figure 3B). Secondly, we studied the expression
303 levels of classical NC-SC lineage markers (46). *NF2*(+/-) and merlin-deficient cell lines,
304 expressed high levels of SC markers such as CDH19, GAP43, MPZ, PLP1 or S100B at 14 days of
305 differentiation, in a similar way to *NF2*(+/+) control lines (Figure 3C), indicating that NC cells
306 were progressing from a precursor state into a committed SC phenotype, probably without
307 reaching a mature myelinating phenotype. Surprisingly, merlin-deficient differentiating SCs
308 maintained the expression of the NC-SC markers up to 30 days in 3D (data not shown).
309 Furthermore, and given that the cells that would make up a schwannoma cell model would be
310 NF2(-/-) cells, we also analysed the *in vitro* NC-SC expression roadmap (45) (Figure 3D). *NF2*(-/-
311) cell lines displayed a very similar NC-SC expression roadmap to that previously determined
312 for *NF2*(+/+) differentiating SCs in 2D (Figure 3D and Supplemental Figure S6) (45).
313
314 **Figure 3. Schwann Cell Differentiation in 3D cultures** (A) Immunochemistry of p75 (green) and
315 S100B (red) after 14 days of SC differentiation, Scale bar, 250µM. (B) PCA analysis (C) Gene
316 expression at day 14 of the 3D SC differentiation protocol (D) *In vitro* NC-SC expression
317 roadmap of the WT line (FiPS, *NF2*(+/+)) in the 2D differentiation protocol and the merlin-
318 deficient lines.

319

320 Overall, we successfully applied 3D SC differentiation conditions to *NF2*(+/-) and *NF2*(-/-) to
321 obtain spheroids expressing NC-SC lineage markers at RNA and protein level. iPSC-derived
322 merlin-deficient differentiating SCs constitute a potential reliable model for VS cells (Figure 4).

323

324 **Figure 4.** Schematic representation of the experimental process.

325

326 **Discussion**

327 The development of bilateral vestibular schwannomas (VS) constitute the most distinctive trait
328 of NF2-related Schwannomatosis (NF2) (7). VS arise from a cell of the Schwann Cell (SC) lineage
329 at the vestibular nerve. SCs from VS can be expanded as primary cultures. However, the small
330 number of passages that primary cells can achieve limits their use in experiments requiring
331 large numbers of cells. In this study we generated *NF2*(+/-) and *NF2*(-/-) iPSC lines by
332 combining direct reprogramming of VS cells and *NF2* gene editing. Specifically, by
333 reprogramming VS cells it was possible to generate two *NF2*(+/-) lines (VSi-25 and VSi-267)
334 derived from two VS (Table 1). Also, a third *NF2*(+/-) cell line (FiPS_CasB2) was generated by
335 CRISPR/Cas9 editing of a control iPSC (FiPS). In addition, by editing of VSi-25 and VSi-267, we
336 obtained two *NF2*(-/-) isogenic cell lines (25-CasD7, 267-CasD2). A third *NF2*(-/-) iPSC line (FiPS-
337 CasH6) was obtained by editing the control FiPS iPSC, also isogenic to *NF2*(+/-) FiPS_CasB2.
338 In contrast to the generation of iPSCs by reprogramming cells derived from other benign
339 peripheral nervous system tumors, like plexiform neurofibromas (42), we were not able to
340 generate genuine iPSCs by reprogramming *NF2*-deficient VS cells. The only *NF2*(-/-) cell line
341 obtained was dependent on the exogenous expression of Yamanaka factors. We hypothesize
342 that *NF2* function is required during the reprogramming process and might be related to its
343 essential role in embryogenesis and early stages of development (19), which is also consistent
344 with the reported essential function of *NF2* in haploid human iPSCs and leukaemia cells

345 (47,48). However, it is possible that using different conditions for the reprogramming of VS
346 cells and/or the maintenance of *NF2*(-/-) iPSCs could produce a different result, so additional
347 evidence is needed to reach a definitive conclusion.
348 Once the cells were in a pluripotent state, we were indeed able to generate *NF2*(-/-) iPSCs
349 through gene editing, as has been recently reported (38). However, in our hands, all three of
350 the *NF2*(-/-) iPSC lines generated required extensive experimental care; showed aberrant
351 colony morphology with a tendency to pile up cells during growth; and were susceptible to
352 spontaneous differentiation in a similar way to the *NF2*(-/-) colonies obtained by reprograming
353 VS cells. Therefore, considering that the origins and the genetic backgrounds of all three *NF2*(-
354 /-) cell lines were different and that the only thing they shared was complete *NF2* inactivation,
355 our results indicate that *NF2* function is responsible for this aberrant phenotype, suggesting it
356 also has an essential role in maintaining pluripotency of diploid cells. However, despite all
357 these limitations, the iPSC lines generated in this study constitute a valuable and unperishable
358 source of cells harbouring single or bi-allelic inactivation of *NF2,* that under adequate culture
359 conditions, could be used as a NF2-cell based model to develop further assays (50).
360 We showed that both *NF2*(+/-) and *NF2*(-/-) iPSCs have the capacity to differentiate towards a
361 NC identity, although *NF2*(-/-) NC cultures exhibited an unstable NC phenotype, with some
362 cells undergoing spontaneous expression of S100B. In addition, we highlight that *NF2*-deficient
363 iPSC-derived NCs required a higher confluence in culture, thus an apparently closer cell-cell
364 contact to maintain NC identity, consistent with the role of merlin in cytoskeleton
365 maintenance and control of proliferation by cell-cell contact inhibition (51–53). Also, in line
366 with these findings, in the process of differentiation of NCs towards SCs, we observed that
367 both *NF2*(+/-) and *NF2*(-/-) cells were easily detached from the cell culture surface, eventually
368 leading to cell death and preventing the generation of SC-like cultures.
369 However, and most importantly, we overcame this limitation by successfully generating
370 NF2(+/-) and NF2(-/-) spheroids growing in suspension as has been previously reported for

371 other SC-based spheroids (45). These spheroids already expressed classical NC-SC markers, as
372 shown by immunostaining, after seven days in SC differentiation medium. In addition,
373 extensive transcriptome analysis of *NF2*(+/-) and *NF2*(-/-) spheroids was performed, evidencing
374 the expression of well characterized NC-SC lineage markers (40). Furthermore, *NF2*(-/-) cells
375 also preserved a previously characterized *in vitro* NC-SC differentiation expression roadmap as
376 control iPSCs (45).
377 Finally, in this study we have generated *NF2*(+/-) and *NF2*(-/-) iPSC lines through
378 reprogramming VS and *NF2* editing. According to our results, the *NF2* gene seems to have a
379 relevant role in the induction and maintenance of pluripotency. iPSCs with different *NF2*
380 genotypes were differentiated into NC cells, although *merlin*-deficient iPSCs exhibited an
381 altered differentiation capacity. *NF2*(-/-) NC cultures showed heterogeneity in the expression
382 of classical NC markers with some cells spontaneously expressing non-NC markers such as
383 S100B. In addition, they were unable to generate SC-like cells in 2D cultures due to a deficient
384 adherence. However, the application of a 3D SC differentiation protocol resulted in the
385 successful generation of *NF2*(+/-) and *NF2*(-/-) spheroids expressing NC-SC lineage markers
386 (Figure 4). These spheroids constitute a valuable resource for the investigation of the biology
387 of NF2-related schwannomas, the study of the impact of *NF2* loss in the molecular
388 pathogenesis of NF2 traits and for the testing of new therapeutic approaches for *NF2*-related
389 tumors. In addition, despite the challenges in the use of *NF2*-deficient iPSCs, this resource
390 could be used to obtain other cell types involved in other NF2-related tumors, such as
391 meningioma- and ependymoma-originating cells.
392
393 **Materials and Methods**
394 All procedures performed were in accordance with the ethical standards of the IGTP
395 Institutional Review Board, which approved this study, and with the 1964 Helsinki declaration

396 and its later amendments. This project was authorised by the "Comisión de Garantías para la
397 Donación y Utilización de Células y Tejidos Humanos, ISCIII")

398 **Patients and Vestibular Schwannoma samples:** tumour samples were obtained from NF2-
399 related SWN patients clinically managed at the Spanish Reference Centre (CSUR) on
400 Phacomatoses HUGTiP-ICO-IGTP, diagnosed according to standard diagnostic criteria (43).
401 Tumour samples were processed as described in Castellanos et al., 2018 (54).

402 **Reprogramming of Vestibular Schwannomas:** between $0.2 \cdot 10^6$-$1 \cdot 10^6$ of VS derived cells were
403 reprogrammed using the CytoTune™-iPS 2.0 Sendai Reprogramming Kit (Thermo Fisher
404 Scientific), a non-integrative cell reprogramming method containing the four Yamanaka factors
405 (OCT4, SOX2, KLF4, and cMYC), according to manufacturer's instructions.

406 **Tumour and iPSC molecular characterization:** genetic analysis was performed using the
407 customized I2HCP panel as previously described (44) or Whole Exome Sequencing (WES). The
408 latter was performed using KAPA HyperCap technology with KAPA HyperExome Probes (Roche)
409 according to manufacturer's instructions and sequenced in a NextSeq instrument (Illumina).
410 Analysis of small nucleotide variants was performed with Mutect2 and annotated with
411 Funcotator (55). Potential SNV and small indels were detected among the original cell lines and
412 the paired CRISPR lines, GATK 4.2.6.1 was used for the whole process (55) (Supplemental
413 Material and Methods). In order to detect *NF2* splicing variants, tumours were studied both at
414 RNA and DNA level. *NF2* variants were validated by Sanger Sequencing. SNP-array analysis was
415 assessed using Illumina HumanOmniExpress v1 BeadChips (730,525 SNPs) according to
416 manufacturers' instructions and as described in Supplemental Material and Methods.

417 **CRISPR/Cas9 gene edition in iPSC lines:** CRISPR/Cas9 editing was performed with the ArciTect
418 ribonucleoprotein (RNP) system (STEMCELL Technologies). The designed sgRNA targeted exon
419 2 of the *NF2* gene (GTACACAATCAAGGACACAG). TransIT-X2® Dynamic Delivery System (Mirus)
420 was used for transfection according to manufacturers' instructions.

421 **iPSC culture:** iPSCs were grown on growth factor-reduced Matrigel (23µg/cm2) (BD
422 Biosciences)-coated 6-well plates and cultured in mTESR Plus medium (STEMCELL
423 Technologies). Splits were performed using Accutase (Merk) and cells were seeded with Rock
424 Inhibitor (1:1000) for 24h (STEMCELL Technologies). When required, visibly differentiated cells
425 were removed manually from the culture of *NF2*(-/-) cells. In this study, the *NF2*(+/+) FiPS line
426 (FiPS Ctrl 1-SV4F-7) was used for all experiments as a control.

427 **Neural Crest (NC) differentiation:** differentiation of iPSCs lines towards NC was performed as
428 previously described in Menendez et al. (2013) (41) with minor modifications (42). $9x10^4$ iPS
429 cells were seeded on matrigel-coated dishes in mTESR Plus medium. The following day, the
430 medium was replaced with Neural Crest Differentiation Media (Supplemental Material and
431 Methods) and was replaced every day. NC were maintained in this medium and split with
432 Accutase when necessary.

433 **Differentiation towards SC in 2D:** to stablish SC differentiation, $0.4x10^6$ NC cells/well were
434 plated onto 0.1mg/mL poly-L-lysine (Sigma) and 4µg/mL laminin (Gibco) and cultured in SC
435 differentiation media (SCDM) (Supplemental Material and Methods) as previously described
436 (42).

437 **Differentiation towards SC in 3D:** NC cells were detached with Accutase and, $2.25 \cdot 10^6$ NC
438 cells/well were seeded onto AggreWell TM800 24-well plates (Stem Cell Technologies) in 2mL
439 SCDM (described above). The medium was changed twice a week removing 1 mL and replacing
440 1 mL of fresh SCDM. On days 7, 14 and 30 spheroids were collected and processed for
441 subsequent analysis.

442 **Flow cytometry:** cells in PBS-0.1% BSA were incubated with p75 primary antibody and
443 subsequently incubated with Alexa Fluor 568 secondary antibody, and Hnk1 primary antibody
444 and detected with Alexa Fluor 488-conjugated secondary antibody. Antibodies were incubated
445 30 min on ice. Cells were analysed by flow cytometry using BD LSR Fortessa SORP and BD FACS
446 Diva 6.2 software.

447 **Immunocytochemistry:** cells or spheroids were fixed in 4% paraformaldehyde in PBS for 15min
448 at room temperature (RT), permeabilized with 0.1%Triton-X 100 in PBS for 10 min at RT,
449 blocked in 10% FBS in PBS for 15 min at RT, and incubated with the indicated antibodies
450 (Supplemental Table M1) overnight at 4°C. Secondary antibodies Alexa Fluor 488 and Alexa
451 Fluor 568 were incubated for 1h at RT. Nuclei were stained with DAPI and images captured
452 using LEICA DMIL6000 and LASAF software.

453 **RNA analysis and heatmaps:** For RNAseq analysis, genome GRCh37.p13 and gene annotation
454 gencode version 19 were used. For the alignment, STAR version 2.7.10a (56)) and QoRTs
455 version 1.3.6 (57) for gene count and general QC were used. For heatmaps, vst normalization
456 from DESeq2 (58) was used. For unsupervised cluster heatmaps, Euclidean metric and Ward
457 method were selected. For barplots in Figure 2, normalization was done by Trimmed Mean of
458 M-values from EdgeR (59) and then RPKMs were calculated for every gene.

459 **Acknowledgements**

460 We thank the HGTP Clinical Services and staff for their collaboration in generating and
461 collecting patient samples and data. We thank the IGTP Flow Cytometry core facility and their
462 staff for their contribution and technical support. We are indebted to all members of the
463 Cytogenetics Platform, Haematology Department at Germans Trias i Pujol Hospital, Catalan
464 Institute of Oncology and Josep Carreras Leukaemia Research Institute (Badalona, Spain) for
465 providing karyotype studies and images. We would like to acknowledge the constant support
466 of the different NF lay associations: *Asociación de Afectados de Neurofibromatosis*, Chromo22
467 and ACNefi. This work has been supported by: *Associació Chromo 22*; The Children's Tumor
468 Foundation (CTF-2019-05-005), the Spanish Association for the NF Affected (AANF), *Fundación*
469 *Proyecto Neurofibromatosis* and the Catalan NF Association (AcNeFi). This study has been
470 funded by the *Instituto de Salud Carlos III* through the project PI20/00215 (Co-funded by
471 European Regional Development Fund "A way to make Europe"), *Fundació La Marató de TV3*
472 (126/C/2020) and the Government of Catalonia (2017 SGR 496).

473

474 **Author contributions**

475 ES, MC and EC conceived and supervised the study and wrote the manuscript that was revised,
476 corrected, and improved by all the authors. NC performed most of the experimental work,
477 analysed the data, generated the figures for the paper and wrote the manuscript. MTM and
478 BG performed bioinformatics analysis. AN, BK, IR, GC and BA performed experimental work.
479 FRR and EA contributed with sample collection. HM, AV, AR and IB provided scientific input. All
480 authors approved the final version of the manuscript.

481

482 **Conflict of interest statement**

483 The authors declare no conflicts of interest.

484

485 **References**

486 1. Evans DGR, Moran A, King A, Saeed S, Gurusinghe N, Ramsden R. Incidence of vestibular
487 schwannoma and neurofibromatosis 2 in the North West of England over a 10-year
488 period: Higher incidence than previously thought. Otol Neurotol. 2005;26(1):93–7.

489 2. Plotkin SR, Messiaen L, Legius E, Pancza P, Avery RA, Blakeley JO, et al. Updated
490 diagnostic criteria and nomenclature for neurofibromatosis type 2 and
491 schwannomatosis: An international consensus recommendation. Genet Med.
492 2022;24(9):1967–77.

493 3. McClatchey AI, Giovannini M. Membrane organization and tumorigenesis - The NF2
494 tumor suppressor, Merlin. Genes Dev. 2005;19(19):2265–77.

495 4. Gladden AB, Hebert AM, Schneeberger EE, McClatchey AI. The NF2 Tumor Suppressor,
496 Merlin, Regulates Epidermal Development through the Establishment of a Junctional
497 Polarity Complex. Dev Cell [Internet]. 2010;19(5):727–39. Available from:
498 http://dx.doi.org/10.1016/j.devcel.2010.10.008

499 5. Petrilli AM, Merlin V, Nf I, Merlin I, Nf O. Role of Merlin / NF2 inactivation in tumor
500 biology. 2016;(December 2014):537–48.
501 6. Evans DG, Bowers NL, Tobi S, Hartley C, Wallace AJ, King AT, et al. Schwannomatosis: A
502 genetic and epidemiological study. J Neurol Neurosurg Psychiatry. 2018 Jun 14;
503 7. Evans DGR, Huson SM, Donnai D, Neary W, Blair V, Teare D, et al. A genetic study of
504 type 2 neurofibromatosis in the United Kingdom. I. Prevalence, mutation rate, fitness,
505 and confirmation of maternal transmission effect on severity. J Med Genet.
506 1992;29(12):841–6.
507 8. Parry DM, Eldridge R, Kaiser-Kupfer MI, Bouzas EA, Pikus A, Patronas N.
508 Neurofibromatosis 2 (NF2): Clinical characteristics of 63 affected individuals and clinical
509 evidence for heterogeneity. Am J Med Genet. 1994;52(4):450–61.
510 9. Baser ME, Makariou E V., Parry DM. Predictors of vestibular schwannoma growth in
511 patients with neurofibromatosis Type 2. J Neurosurg. 2002 Feb;96(2):217–22.
512 10. Forde C, King AT, Rutherford SA, Hammerbeck-Ward C, Lloyd SK, Freeman SR, et al.
513 Disease course of neurofibromatosis type 2: A 30-year follow-up study of 353 patients
514 seen at a single institution. Neuro Oncol. 2021;23(7):1113–24.
515 11. Ragge NK, Baser ME, Klein J, Nechiporuk A, Sainz J, Pulst SM, et al. Ocular abnormalities
516 in neurofibromatosis 2. Am J Ophthalmol [Internet]. 1995;120(5):634–41. Available
517 from: http://dx.doi.org/10.1016/S0002-9394(14)72210-X
518 12. Plana-Pla A, Bielsa-Marsol I, Carrato-Moñino C. Diagnostic and Prognostic Relevance of
519 the Cutaneous Manifestations of Neurofibromatosis Type 2. Actas Dermosifiliogr.
520 2017;108(7):630–6.
521 13. Hexter A, Jones A, Joe H, Heap L, Smith MJ, Wallace AJ, et al. Clinical and molecular
522 predictors of mortality in neurofibromatosis 2: A UK national analysis of 1192 patients. J
523 Med Genet. 2015;52(10):699–705.
524 14. Dirks MS, Butman JA, Kim HJ, Wu T, Morgan K, Tran AP, et al. Long-term natural history

525 of neurofibromatosis Type 2-associated intracranial tumors: Clinical article. J
526 Neurosurg. 2012 Jul;117(1):109–17.
527 15. Peyre M, Goutagny S, Bah A, Bernardeschi D, Larroque B, Sterkers O, et al. Conservative
528 management of bilateral vestibular schwannomas in neurofibromatosis type 2 patients:
529 Hearing and tumor growth results. Neurosurgery. 2013 Jun;72(6):907–13.
530 16. Baser ME, Mautner VF, Parry DM, Evans DGR. Methodological issues in longitudinal
531 studies: Vestibular schwannoma growth rates in neurofibromatosis 2. Vol. 42, Journal
532 of Medical Genetics. BMJ Publishing Group; 2005. p. 903–6.
533 17. Lloyd SKW, Evans DGR. Neurofibromatosis type 2 (NF2): Diagnosis and management
534 [Internet]. 1st ed. Vol. 115, Handbook of Clinical Neurology. Elsevier B.V.; 2013. 957–
535 967 p. Available from: http://dx.doi.org/10.1016/B978-0-444-52902-2.00054-0
536 18. Plotkin SR, Duda DG, Muzikansky A, Allen J, Blakeley J, Rosser T, et al. Multicenter,
537 prospective, phase II and biomarker study of high-dose bevacizumab as induction
538 therapy in patients with neurofibromatosis type 2 and progressive vestibular
539 schwannoma. J Clin Oncol. 2019;37(35):3446–54.
540 19. McClatchey AI, Saotome I, Ramesh V, Gusella JF, Jacks T. The Nf2 tumor suppressor
541 gene product is essential for extraembryonic development immediately prior to
542 gastrulation. Genes Dev. 1997;11(10):1253–65.
543 20. Behling F, Bersali I, Santacroce A, Hempel J, Kandilaris K, Schittenhelm J, et al. Transition
544 of a vestibular schwannoma to a malignant peripheral nerve sheath tumor with loss of
545 H3K27 trimethylation after radiosurgery—a case report and review of the literature.
546 Neurosurg Rev [Internet]. 2022;45(1):915–22. Available from:
547 https://doi.org/10.1007/s10143-021-01620-3
548 21. Wu L, Vasilijic S, Sun Y, Chen J, Landegger LD, Zhang Y, et al. Losartan prevents tumor-
549 induced hearing loss and augments radiation efficacy in NF2 schwannoma rodent
550 models [Internet]. Vol. 13, Sci. Transl. Med. 2021. Available from:

551 https://www.science.org

552 22. Karajannis MA, Legault G, Hagiwara M, Ballas MS, Brown K, Nusbaum AO, et al. Phase II
553 trial of lapatinib in adult and pediatric patients with neurofibromatosis type 2 and
554 progressive vestibular schwannomas. Neuro Oncol. 2012 Sep;14(9):1163–70.

555 23. Osorio DS, Hu J, Mitchell C, Allen JC, Stanek J, Hagiwara M, et al. Effect of lapatinib on
556 meningioma growth in adults with neurofibromatosis type 2. J Neurooncol. 2018 Sep
557 1;139(3):749–55.

558 24. Welling DB, Collier KA, Burns SS, Oblinger JL, Shu E, Miles-Markley BA, et al. Early phase
559 clinical studies of AR-42, a histone deacetylase inhibitor, for neurofibromatosis type 2-
560 associated vestibular schwannomas and meningiomas. Laryngoscope Investig
561 Otolaryngol. 2021 Oct 1;6(5):1008–19.

562 25. McClatchey AI, Saotome I, Mercer K, Crowley D, Gusella JF, Bronson RT, et al. Mice
563 heterozygous for a mutation at the Nf2 tumor suppressor locus develop a range of
564 highly metastatic tumors. Genes Dev. 1998;12(8):1121–33.

565 26. Stemmer-Rachamimov AO, Louis DN, Nielsen GP, Antonescu CR, Borowsky AD, Bronson
566 RT, et al. Comparative pathology of nerve sheath tumors in mouse models and humans.
567 Cancer Res. 2004;64(10):3718–24.

568 27. Giovannini M, Robanus-Maandag E, Van Der Valk M, Niwa-Kawakita M, Abramowski V,
569 Goutebroze L, et al. Conditional biallelic Nf2 mutation in the mouse promotes
570 manifestations of human neurofibromatosis type 2 [Internet]. 2000. Available from:
571 www.genesdev.org

572 28. Ren Y, Chari DA, Vasilijic S, Welling DB, Stankovic KM. New developments in
573 neurofibromatosis type 2 and vestibular schwannoma. Neuro-Oncology Adv.
574 2021;3(1):1–13.

575 29. Dilwali S, Patel PB, Roberts DS, Basinsky GM, Harris GJ, Emerick KS, et al. Primary
576 culture of human Schwann and schwannoma cells: Improved and simplified protocol.

577 Hear Res. 2014;315:25–33.

578 30. Rosenbaum C, Kluwe L, Mautner VF, Friedrich RE, Mü HW, Hanemann CO. Isolation and
579 Characterization of Schwann Cells from Neurofibromatosis Type 2 Patients. 1998.

580 31. Xue L, He W, Wang Z, Chen H, Wang Z, Wu H. Characterization of a newly established
581 schwannoma cell line from a sporadic vestibular schwannoma patient. Am J Transl Res.
582 2021;13(8):8787–803.

583 32. Hung G, Rhim JS, Slattery W, Lim D. Establishment and characterization of a
584 schwannoma cell line from a patient with neurofibromatosis 2. Vol. 20, INTERNATIONAL
585 JOURNAL OF ONCOLOGY. 2002.

586 33. Takahashi K, Yamanaka S. Induction of Pluripotent Stem Cells from Mouse Embryonic
587 and Adult Fibroblast Cultures by Defined Factors. 2006;2:663–76.

588 34. Shi Y, Inoue H, Wu JC, Yamanaka S. Induced pluripotent stem cell technology: A decade
589 of progress. Vol. 16, Nature Reviews Drug Discovery. Nature Publishing Group; 2017. p.
590 115–30.

591 35. Papapetrou EP. Patient-derived induced pluripotent stem cells in cancer research and
592 precision oncology. Vol. 22, Nature Medicine. Nature Publishing Group; 2016. p. 1392–
593 401.

594 36. Raya Á, Rodríguez-Piz I, Guenechea G, Vassena R, Navarro S, Barrero MJ, et al. Disease-
595 corrected haematopoietic progenitors from Fanconi anaemia induced pluripotent stem
596 cells. Nature. 2009;460(7251):53–9.

597 37. Mungenast AE, Siegert S, Tsai LH. Modeling Alzheimer's disease with human induced
598 pluripotent stem (iPS) cells. Mol Cell Neurosci [Internet]. 2016;73:13–31. Available
599 from: http://dx.doi.org/10.1016/j.mcn.2015.11.010

600 38. Nourbakhsh A, Gosstola NC, Fernandez-Valle C, Dykxhoorn DM, Liu XZ. Characterization
601 of UMi031-A-2 inducible pluripotent stem cell line with a neurofibromatosis type 2-
602 associated mutation. Stem Cell Res. 2021 Aug 1;55.

603 39. Ishi Y, Era T, Yuzawa S, Okamoto M, Sawaya R, Motegi H, et al. Analysis of induced
604 pluripotent stem cell clones derived from a patient with mosaic neurofibromatosis
605 type 2. Vol. 188, American journal of medical genetics. Part A. United States; 2022. p.
606 1863–7.
607 40. Jessen KR, Mirsky R. The origin and development of glial cells in peripheral nerves. Nat
608 Rev Neurosci. 2005;6(9):671–82.
609 41. Menendez L, Kulik MJ, Page AT, Park SS, Lauderdale JD, Cunningham ML, et al. Directed
610 differentiation of human pluripotent cells to neural crest stem cells. Nat Protoc. 2013
611 Jan;8(1):203–12.
612 42. Carrió M, Mazuelas H, Richaud-Patin Y, Gel B, Terribas E, Rosas I, et al. Reprogramming
613 Captures the Genetic and Tumorigenic Properties of Neurofibromatosis Type 1
614 Plexiform Neurofibromas. Stem Cell Reports. 2019;12.
615 43. Baser ME, Friedman JM, Wallace AJ, Ramsden RT, Joe H, Evans DGR. Evaluation of
616 clinical diagnostic criteria for neurofibromatosis 2. Neurology. 2002 Dec;59(11):1759–
617 65.
618 44. Castellanos E, Gel B, Rosas I, Tornero E, Santín S, Pluvinet R, et al. A comprehensive
619 custom panel design for routine hereditary cancer testing: Preserving control,
620 improving diagnostics and revealing a complex variation landscape. Sci Rep. 2017;7.
621 45. Mazuelas H, Magallón-Lorenz M, Fernández-Rodríguez J, Uriarte-Arrazola I, Richaud-
622 Patin Y, Terribas E, et al. Modeling iPSC-derived human neurofibroma-like tumors in
623 mice uncovers the heterogeneity of Schwann cells within plexiform neurofibromas. Cell
624 Rep [Internet]. 2022 Feb;38(7):110385. Available from:
625 https://linkinghub.elsevier.com/retrieve/pii/S2211124722001061
626 46. Jessen KR, Mirsky R, Lloyd AC. Schwann cells: Development and role in nerve repair.
627 Cold Spring Harb Perspect Biol. 2015 Jul 1;7(7):1–15.
628 47. Yilmaz A, Peretz M, Aharony A, Sagi I, Benvenisty N. Defining essential genes for human

629 pluripotent stem cells by CRISPR-Cas9 screening in haploid cells. Nat Cell Biol [Internet].
630 2018;20(5):610–9. Available from: http://dx.doi.org/10.1038/s41556-018-0088-1
631 48. Blomen VA, Májek P, Jae LT, Bigenzahn JW, Nieuwenhuis J, Staring J, et al. Gene
632 essentiality and synthetic lethality in haploid human cells. Science (80-).
633 2015;350(6264):1092–6.
634 49. Nourbakhsh A, Gosstola NC, Fernandez-Valle C, Dykxhoorn DM, Liu XZ. Characterization
635 of UMi031-A-2 inducible pluripotent stem cell line with a neurofibromatosis type 2-
636 associated mutation. Stem Cell Res [Internet]. 2021;55(June):102474. Available from:
637 https://doi.org/10.1016/j.scr.2021.102474
638 50. Rowe RG, Daley GQ. Induced pluripotent stem cells in disease modelling and drug
639 discovery. Vol. 20, Nature Reviews Genetics. Nature Publishing Group; 2019. p. 377–88.
640 51. Curto M, McClatchey AI. Nf2/Merlin: A coordinator of receptor signalling and
641 intercellular contact. Br J Cancer. 2008;98(2):256–62.
642 52. Curto M, Cole BK, Lallemand D, Liu CH, McClatchey AI. Contact-dependent inhibition of
643 EGFR signaling by Nf2/Merlin. J Cell Biol. 2007 Jun 4;177(5):893–903.
644 53. Catasús N, Rosas I, Bonache S, Negro A, Torres-Martin M, Plana-Pla A, et al. Antisense
645 oligonucleotides targeting exon 11 are able to partially rescue the NF2-related
646 schwannomatosis phenotype in vitro. Mol Ther - Nucleic Acids [Internet].
647 2022;30(December):493–505. Available from:
648 https://doi.org/10.1016/j.omtn.2022.10.026
649 54. Castellanos E, Plana A, Carrato C, Carri M, Rosas I, Amilibia E, et al. Early genetic
650 diagnosis of neurofibromatosis type 2 from skin plaque plexiform schwannomas in
651 childhood. JAMA Dermatology. 2018 Mar 1;154(3):341–6.
652 55. Van der Auwera GA, O'Connor BD. Genomics in the Cloud: Using Docker, GATK, and
653 WDL in Terra [Internet]. O'Reilly Media; 2020. Available from:
654 https://books.google.es/books?id=vsXaDwAAQBAJ

655 56. Dobin A, Davis CA, Schlesinger F, Drenkow J, Zaleski C, Jha S, et al. STAR: ultrafast
656 universal RNA-seq aligner. Bioinformatics. 2013 Jan;29(1):15–21.
657 57. Hartley SW, Mullikin JC. QoRTs: a comprehensive toolset for quality control and data
658 processing of RNA-Seq experiments. BMC Bioinformatics. 2015 Jul;16(1):224.
659 58. Love MI, Huber W, Anders S. Moderated estimation of fold change and dispersion for
660 RNA-seq data with DESeq2. Genome Biol. 2014;15(12):550.
661 59. Robinson MD, McCarthy DJ, Smyth GK. edgeR: a Bioconductor package for differential
662 expression analysis of digital gene expression data. Bioinformatics. 2010 Jan;26(1):139–
663 40.
664
665

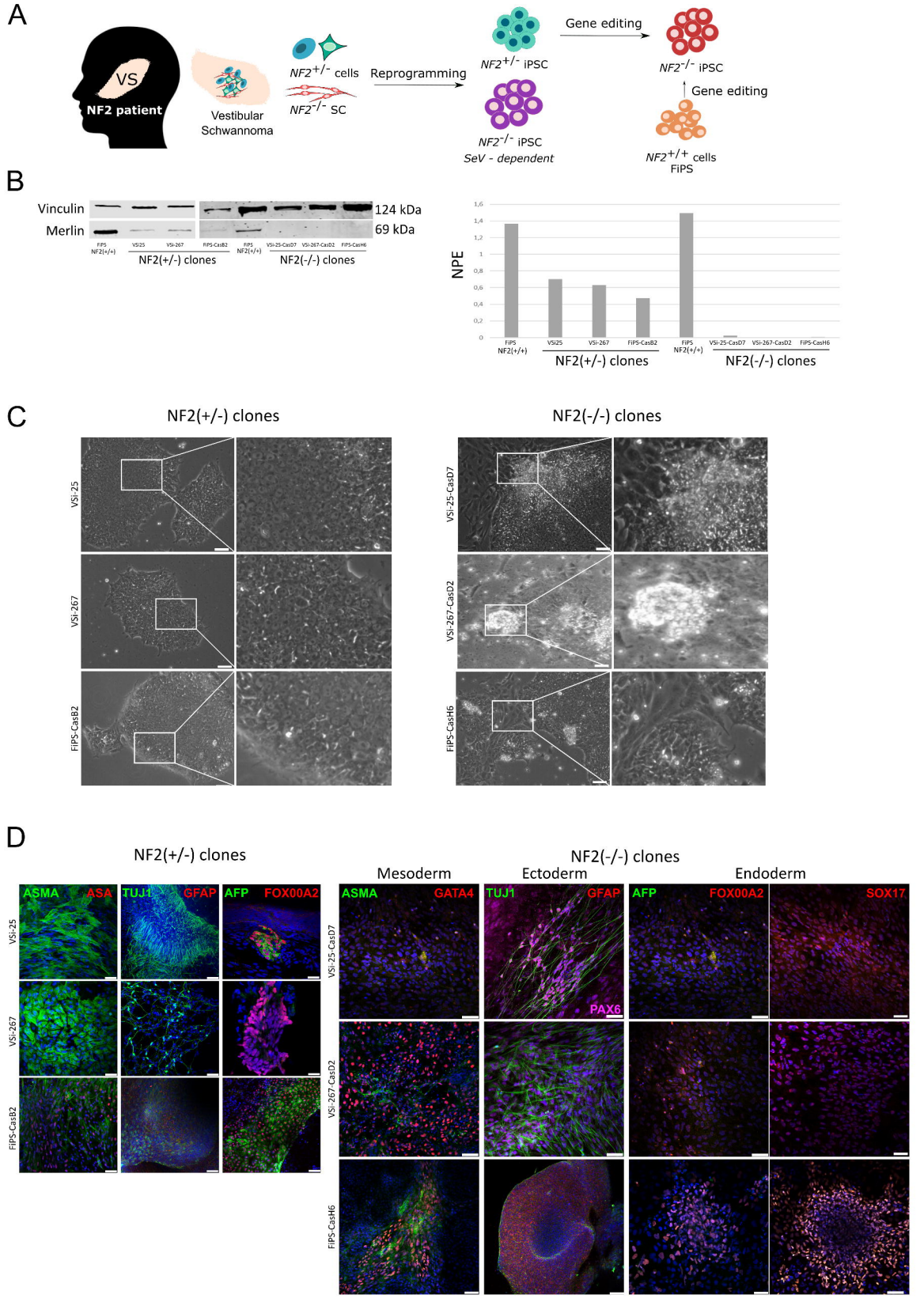
A
VS
NF2 patient
Vestibular Schwannoma
NF2+/- cells
NF2-/- SC
Reprogramming
NF2+/- iPSC
NF2-/- iPSC
SeV - dependent
Gene editing
NF2-/- iPSC
Gene editing
NF2+/+ cells
FiPS
B
Vinculin
Merlin
124 kDa
69 kDa
FiPS NF2(+/+)
VSi25
VSi-267
FiPS-CasB2
FiPS NF2(+/+)
VSi-25-CasD7
VSi-267-CasD2
FiPS-CasH6
NF2(+/-) clones
NF2(-/-) clones
NPE
1,6
1,4
1,2
1
0,8
0,6
0,4
0,2
0
NF2(+/-) clones
NF2(-/-) clones
C
NF2(+/-) clones
NF2(-/-) clones
VSi-25
VSi-267
FiPS-CasB2
VSi-25-CasD7
VSi-267-CasD2
FiPS-CasH6
D
NF2(+/-) clones
NF2(-/-) clones
Mesoderm
Ectoderm
Endoderm
ASMA
ASA
TUJ1
GFAP
AFP
FOX00A2
ASMA
GATA4
TUJ1
GFAP
PAX6
AFP
FOX00A2
SOX17
VSi-25
VSi-267
FiPS-CasB2
VSi-25-CasD7
VSi-267-CasD2
FiPS-CasH6

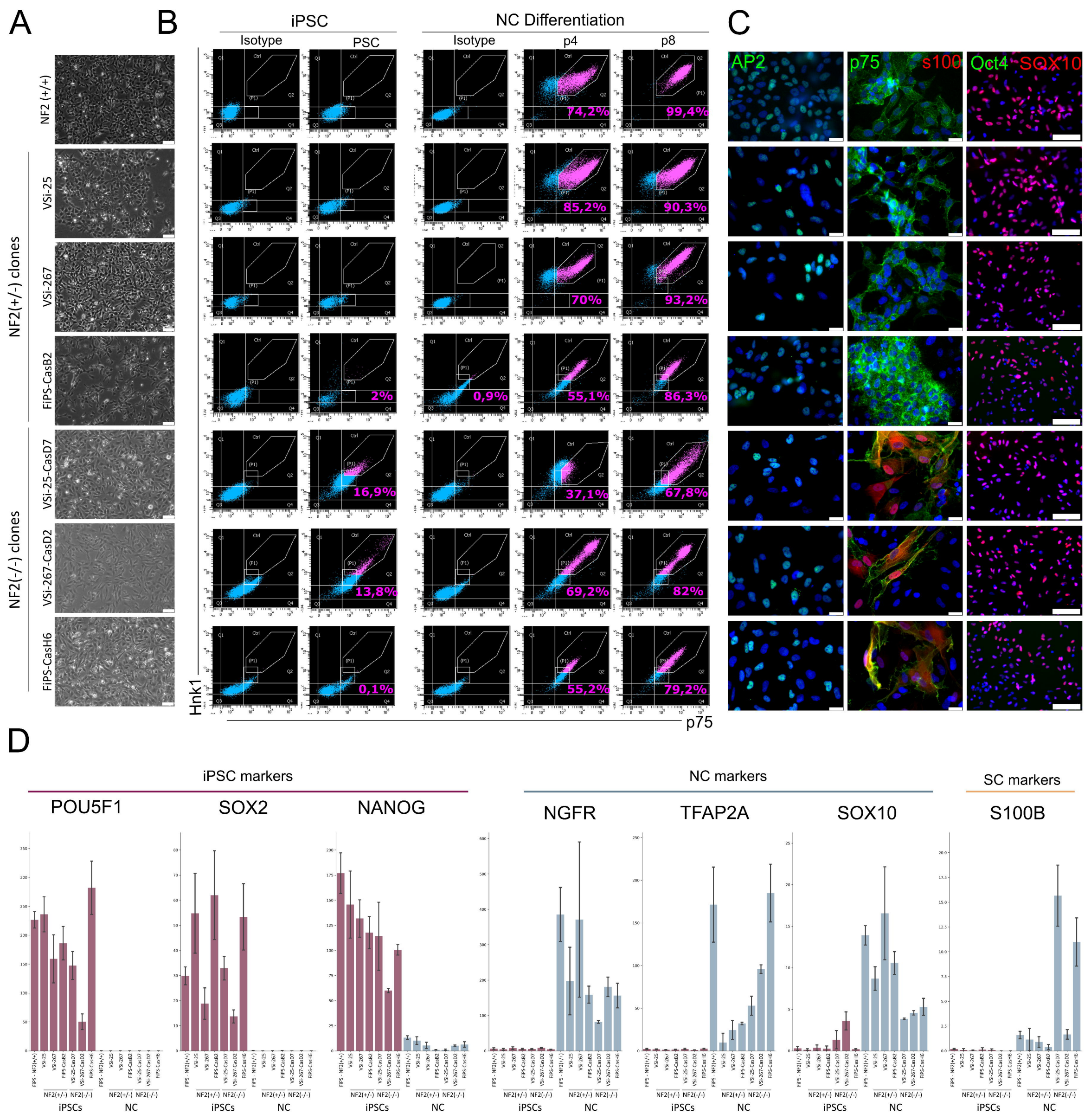
A
B
iPSC
NC Differentiation
Isotype
PSC
Isotype
p4
p8
NF2 (+/+)
NF2(+/-) clones
VSi-25
VSi-267
FiPS-CasB2
NF2(-/-) clones
VSi-25-CasD7
VSi-267-CasD2
FiPS-CasH6
74,2%
99,4%
85,2%
90,3%
70%
93,2%
2%
0,9%
55,1%
86,3%
16,9%
37,1%
67,8%
13,8%
69,2%
82%
0,1%
55,2%
79,2%
Hnk1
p75
C
AP2
p75
s100
Oct4
SOX10
D
iPSC markers
NC markers
SC markers
POU5F1
SOX2
NANOG
NGFR
TFAP2A
SOX10
S100B
iPSCs
NC

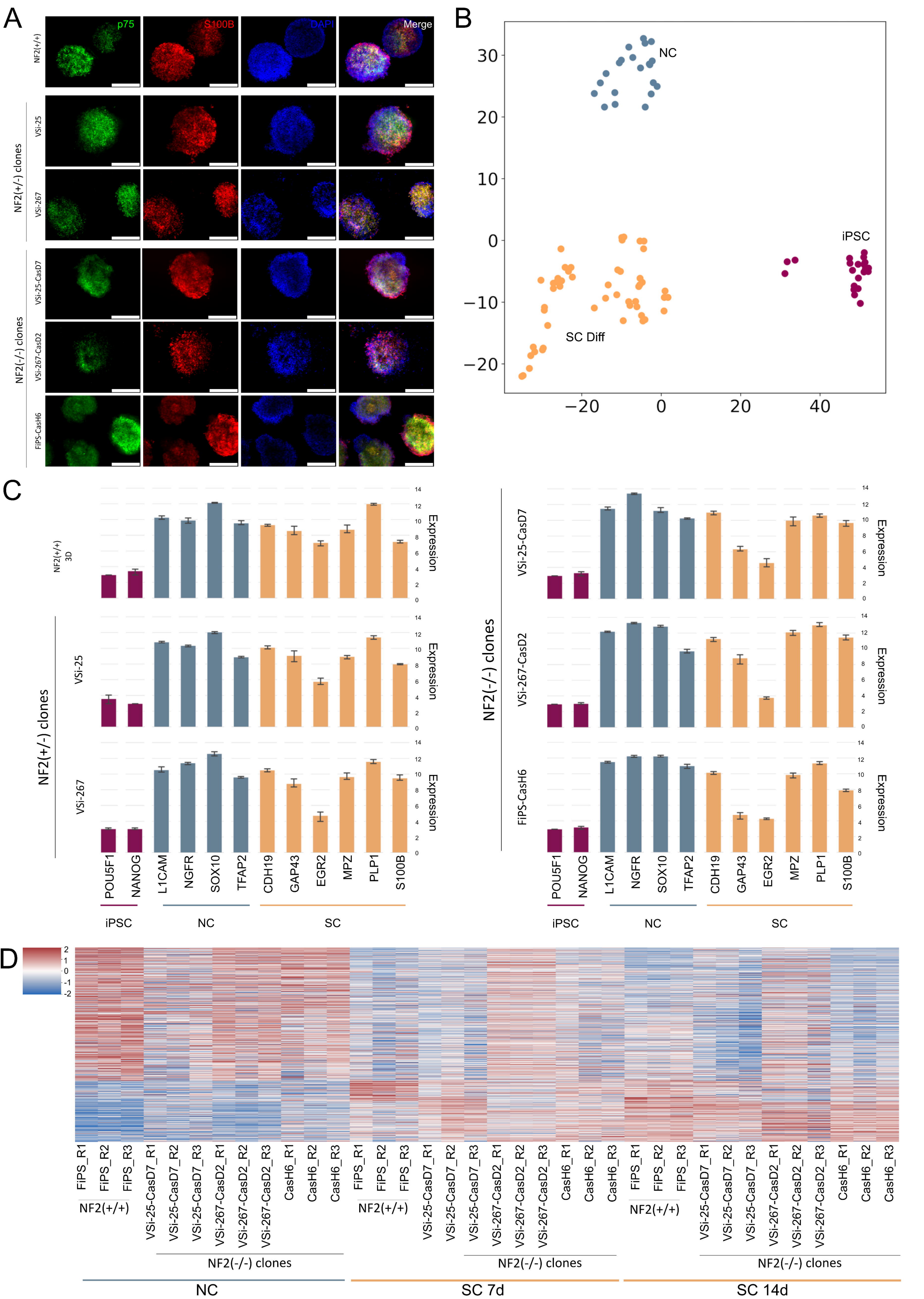
A
p75
S100B
DAPI
Merge
NF2(+/+)
NF2(+/-) clones
VSi-25
VSi-267
NF2(-/-) clones
VSi-25-CasD7
VSi-267-CasD2
FiPS-CasH6
B
NC
iPSC
SC Diff
C
NF2(+/+) 3D
NF2(+/-) clones
NF2(-/-) clones
Expression
POU5F1
NANOG
L1CAM
NGFR
SOX10
TFAP2
CDH19
GAP43
EGR2
MPZ
PLP1
S100B
iPSC
NC
SC
D
NF2(+/+)
NF2(-/-) clones
NC
SC 7d
SC 14d

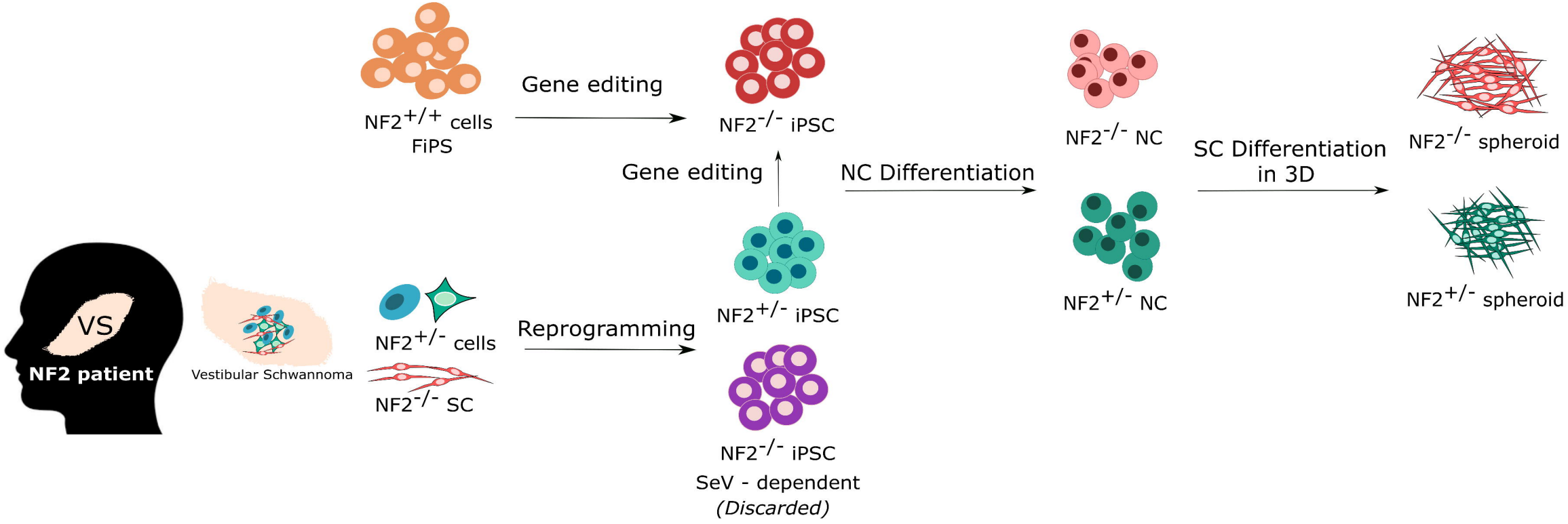
VS
NF2 patient
Vestibular Schwannoma
NF2+/+ cells
FiPS
Gene editing
NF2-/- iPSC
Gene editing
NF2+/- cells
NF2-/- SC
Reprogramming
NF2+/- iPSC
NF2-/- iPSC
SeV - dependent
(Discarded)
NC Differentiation
NF2-/- NC
NF2+/- NC
SC Differentiation
in 3D
NF2-/- spheroid
NF2+/- spheroid